

2

Conf-930269--16

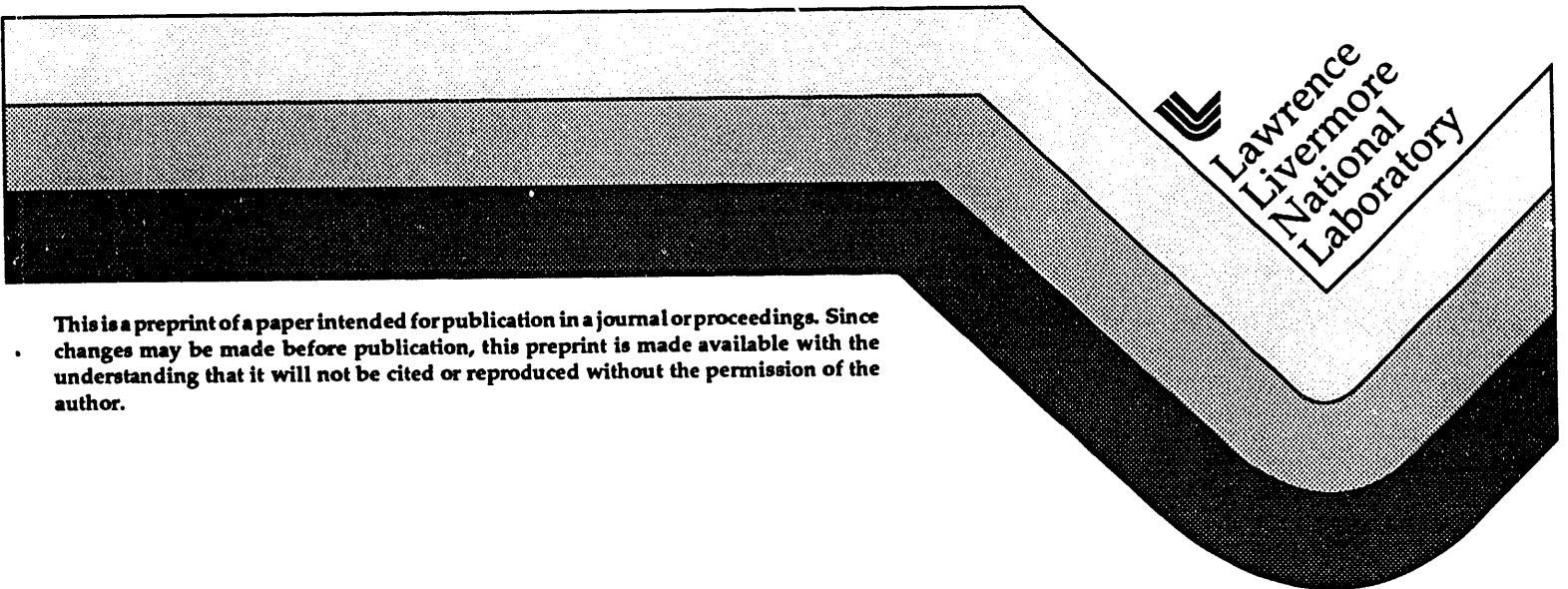
UCRL-JC-112245
PREPRINT

**PIC Space-Charge Emission with
Finite Δt and Δz**

Dennis W. Hewett and Yu-Jiuan Chen

**This paper was prepared for submittal to the
Proceedings of the Computational Accelerator
Physics Conference, Pleasanton, California
February 22-26, 1993**

February 22, 1993



This is a preprint of a paper intended for publication in a journal or proceedings. Since changes may be made before publication, this preprint is made available with the understanding that it will not be cited or reproduced without the permission of the author.

DISCLAIMER

This document was prepared as an account of work sponsored by an agency of the United States Government. Neither the United States Government nor the University of California nor any of their employees, makes any warranty, express or implied, or assumes any legal liability or responsibility for the accuracy, completeness, or usefulness of any information, apparatus, product, or process disclosed, or represents that its use would not infringe privately owned rights. Reference herein to any specific commercial product, process, or service by trade name, trademark, manufacturer, or otherwise, does not necessarily constitute or imply its endorsement, recommendation, or favoring by the United States Government or the University of California. The views and opinions of authors expressed herein do not necessarily state or reflect those of the United States Government or the University of California, and shall not be used for advertising or product endorsement purposes.

PIC Space-Charge Emission with Finite Δt and Δz *

Dennis W. Hewett and Yu-Jiuan Chen
Lawrence Livermore National Laboratory
University of California
Livermore, California 94550

ABSTRACT

A new algorithm for space charge emission has been developed to provide the correct (to a few percent) Child-Langmuir steady-state current limits as the number of mesh points in the voltage gap drops to $O(10)$. Further, the transient behavior of such flows compares well with idealized, analytic cases, lending confidence as we extend these algorithms into full RZ geometry with curved emitting surfaces to investigate transient characteristics of realistic injector designs.

INTRODUCTION

Charged particle source physics has a wide range of applications. Of particular interest are new applications in plasma-aided manufacturing where ions essential to the process are extracted from a plasma. This same physics is applicable to the heavy ion source, a crucial part of Heavy Ion Fusion HIF. The common theme is the extraction of the desired ion species from a region of neutral or quasi-neutral material by an external voltage. The dividing line between the beam and quasineutral regions can be viewed as a Space-Charge-Emitting Surface (SCES) that can be modeled in a simulation as a boundary condition. We hold this surface at a fixed potential and assume it to be able to deliver all the particles or charge necessary to reduce the surface normal electric field to zero. The numerical boundary must emit these particles such that they may be extracted with little transverse temperature and thus quickly achieve the anisotropic velocity profiles that are an essential feature of many applications. In practice, building such a numerical boundary condition is not difficult if we use of order 100-200 grid points in the gap between the anode and cathode (called

* Work performed under the auspices of the U.S. Department of Energy by Lawrence Livermore National Laboratory under contract W-7405-ENG-48.

the A-K gap) and a sufficiently small time step so that the fastest particles do not travel more than a cell in Δt . As may be surmised, we do not have the luxury of carefully resolving the SCES in codes that are to be used frequently as design tools. We are required by computational demands to use very large space steps Δz and large time steps Δt .

Electrode design in such sources is also critical to the overall performance. Steady state codes, such as EGUN¹, can provide excellent predictive capabilities for the steady-state flow characteristics of a given configuration. However, in short pulse operation in which the control of beam transient behavior is essential, time-dependent acceleration and focusing voltages add yet another dimension to the problem. Only time-dependent simulation can provide the detailed information needed to assess the effect of voltage waveforms on the beam bunch shape. This information is essential to the design of such low-emittance, short-pulse source electrode configurations and to the design of the associated pulse power supplies.

In this paper we describe such a time-dependent code and concentrate on the numerical treatment of the SCES. We utilize the external and internal electrode structure specification capabilities of the time-dependent, axisymmetric RZ PIC code, GYMNOS². Since we will not generally have the luxury of carefully resolving the SCES region, We have developed a space-charge-emission algorithm that allows us to use large space and time steps and satisfies three criteria. First, it must provide steady-state currents to within a few percent of *both* the well-proven EGUN result *and* the experimental measurement even as the resolution becomes marginal. Second, agreement is also required between GYMNOS, EGUN, and the experiment in steady-state normalized emittance values. Finally, we expect GYMNOS to provide detailed agreement with the few beam transient test cases that can be found analytically.

GEOMETRIC PROPERTIES OF GYMNOS

GYMNOS stores all quantities on the corners of a regular uniform RZ mesh. The boundaries of all structures, internal or external, also are assumed to lie on these corners. In a simple electrostatic case, a charge density ρ is accumulated from the PIC ion representation on all mesh points — taking care to use the correct reduced volume when finding ρ at a mesh point that is on a structure boundary. Given the instantaneous ρ , we then solve for the

consistent electrostatic potential ϕ on *all* the mesh points, including those that represent the space-charge-emitting SCES. On the SCES we specify ϕ (typically $\phi = 0$). At most points \mathbf{E} is obtained by central differencing. On the SCES boundary, since we know ϕ and ρ at all points, we can reconstruct the potential value ϕ_{in} just inside the SCES structure from the ϕ value *on* the SCES, the one just outside the SCES, and the ρ at the point in question. Finite differencing for \mathbf{E} at this point using ϕ_{in} gives a second-order approximation for the electric field on the SCES.

IMPLEMENTATION OF THE SCES BOUNDARY

We now add the additional physics that characterizes a SCES; charge is emitted until the normal \mathbf{E} is also zero. We use this condition to determine how much charge would have to be emitted each time step to bring the surface field described above back to the physics-required zero. The condition is simple: the surface normal \mathbf{E} is equated to an induced surface charge σ that, multiplied by the surface area represented by that node, just gives the space charge that should be emitted this time step.

We now describe our implementation of this straightforward algorithm together with numerical tests that have allowed us to tune the algorithm so that it provides remarkable agreement with very coarse finite difference representations. Given the above prescription for the surface normal \mathbf{E} and thus the charge induced from the surface for emission, we fill a reservoir at each mesh point and emit particles from the reservoir until it no longer exceeds the charge carried by each simulation particle. (Other approaches use variable particle weights so as to emit constant *numbers* of particles/cell/ Δt ; so far our results seem more than adequate using uniform weighting.)

In the limit of a small time step and many spacial grid points between anode and cathode, many straightforward algorithms can provide adequate results. We now present the test results that show that one algorithm continues to work well as resolution degrades and seems to be robust enough to also work as the SCES is generalized to a curved surface. The method is to place randomly as many particles as can be extracted from the reservoir randomly in the first half cell outside the SCES, and to give these particles a normal velocity $\mathbf{u}_{\text{norm}} = 2\Delta t q \mathbf{E}_{\text{norm}}/m$. This expression for u_{norm} is derived from the condition that the normal force times

rate at which the particle gains kinetic energy, i.e.,

$$qE_{\text{norm}}u_{\text{norm}} = mu_{\text{norm}}^2/2\Delta t \quad , \quad (1)$$

where the electric field is evaluated one-half cell outside of the SCES. Empirically, we have found that a very good choice is to evaluate the electric field one-half cell outside the SCES.

NUMERICAL TESTS OF THE SCES BOUNDARY

The simulation tests that lead us to these choices were an 1-D potassium ($A=39$) diode studies with a gap distance of 1.6 cm and a voltage of -6.56 kV in which we varied the number of mesh points in the gap. The Child-Langmuir current for a such diode is 0.057 mA. Shown in Fig. 1 are 1D cases with 240 mesh points in the A-K gap in Fig 1a and the corresponding run with only 8 mesh points in Fig. 1b. We have shown the steady-state v_z vs. z phase space in which the random loading in the first half cell outside of z_{min} is very apparent in the coarse mesh case. Nonetheless the total current for both the 240 mesh point case and the 8 mesh point case is 0.057 mA, within PIC noise, as predicted by the Child-Langmuir law. The time step is a relatively small $\Delta t = 0.5$ ns in both cases.

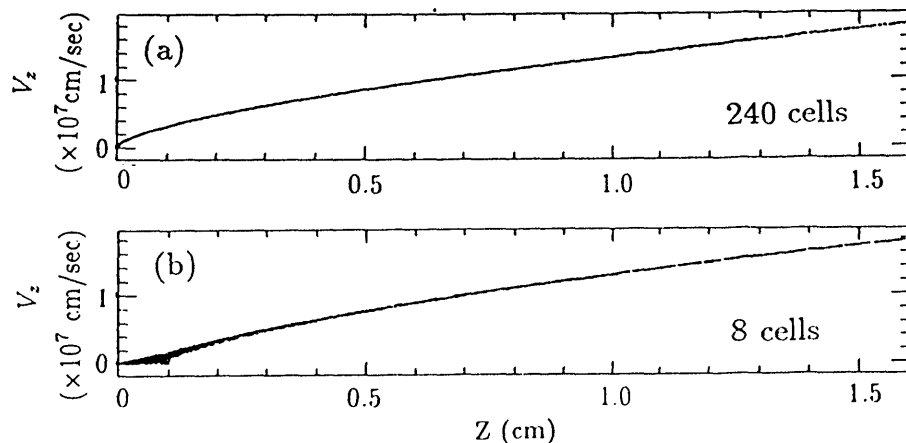


Fig. 1 The v_z vs. z phase spaces for the 1-D diode with (a) 240 and (b) 8 mesh points in the A-K gap.

Since one of the purposes of the time-dependent approach is to study the effect of transients, we show in Fig. 2 the simulation results of the same 1-D potassium diode using the A-K voltage

waveform

$$\begin{aligned} \phi(t) &= \left[\frac{4}{3} \frac{t}{t_{\text{rise}}} - \frac{1}{3} \left(\frac{t}{t_{\text{rise}}} \right)^4 \right] \phi_0, & t \leq t_{\text{rise}} \quad , \\ \phi(t) &= \phi_0, & t > t_{\text{rise}} \quad . \end{aligned} \quad (2)$$

Using the same time step as in Fig. 1 and 8 mesh points in the A-K gap, the steady current values in both Figs. 2a and 2b are the same 0.057 mA since the voltages and gap distances are the same as that of the Fig. 1 tests. For the case in Fig. 2a, the waveform used in the simulation has the rise time t_{rise} equal to the transit time, t_{trans} , for an ion to cross the A-K gap, i.e., the so-called Lampel and Tiefenback voltage waveform³. By using this voltage waveform, we obtained the predicted constant current profile for the front end and the flat-top of the beam pulse. When $t_{\text{rise}} < t_{\text{trans}}$, we expect the same asymptotic Child-Langmuir current at the flat-top portion of the beam pulse led by a higher current during the rise time. In the case $t_{\text{rise}} = 150$ ns, the current during the rise time is estimated to be roughly 0.08 mA. Our result for this situation is shown in Fig. 2b. The degree to which our simulation results agree with analytic predictions in both cases gives us confidence that we can achieve useful results in more complicated geometries where we are forced to work with limited spatial resolution.

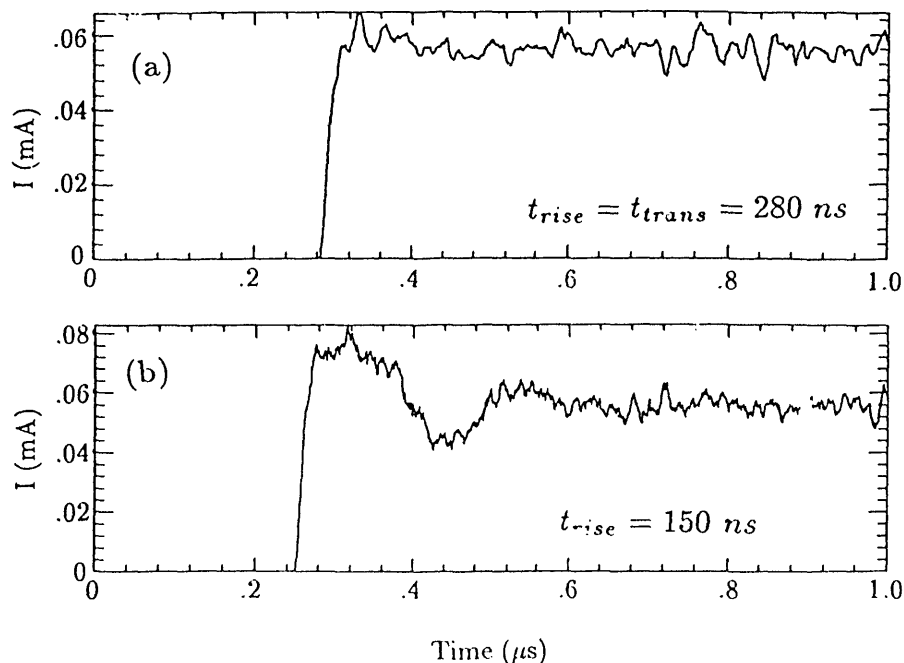


Fig. 2 The current profile calculated by GYMNOS when the A-K gap voltage waveform's rise time is (a) equal to and (b) less than the ion transit time, respectively.

We have used GYMNOS to study the axisymmetric LBL HIF electrostatic column injector. In Fig. 3 we show a case with a current valve mesh^{4,5}, used to control the beam pulse. Only 8 mesh points across the gap between the emitting surface and the current valve were used in the simulations to resolve the z -variations of the electric field. The comparison of current, normalized emittance, beam envelope radius, and beam divergence from GYMNOS simulation, experiment⁶, and EGUN are given in Table I. The EGUN calculations were done from the immediately downstream side of the current valve mesh to the emittance diagnostics location by Henestroza⁷. To include finite temperature effects in the EGUN calculations, the initial transverse beam velocity distributions at the current valve location must be assumed. Several "reasonable" distribution functions, all with the same transverse temperature as the GYMNOS runs, were chosen to characterize the emittance that is representative of this geometry. The result is the range of emittances that are given for EGUN in Table 1. Figure 3 shows that the beam radius is comparable to the electrodes' aperture size. Hence, the beam experiences a large nonlinear external field and its normalized beam emittance grows from its intrinsic value of 0.05 mm-mr at the source to 0.25 mm-mr at the emittance diagnostics location.

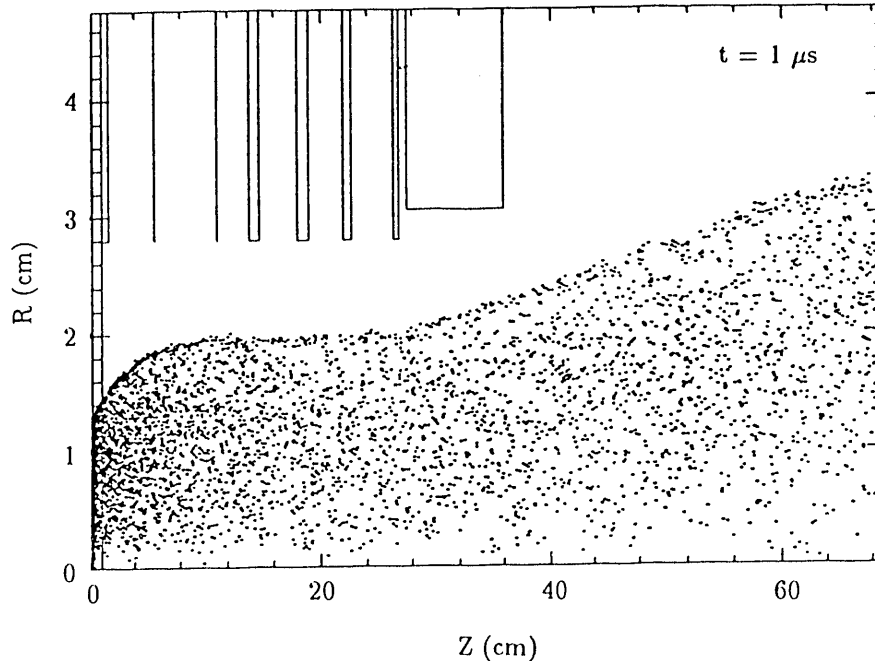


Fig.3 The LBL HIF injector with a current valve

Table I The LBL HIF injector with a current valve

	GYMNOS	EXP ⁶	EGUN ⁷
Current (mA)	82	80	80
Normalized emittance (mm-mr)	.26	.25	0.07-0.2
Beam radius (mm)	32.5	31.2	31.0
Beam divergence (mr)	34.5	38.4	36.0

The GYMNOS result of the same configuration without the current valve and with the same mesh size in the z direction is shown in Fig. 4. When the current valve mesh was removed, the voltage of the first electrode (at $z=1.2$ cm in Fig. 4) was the same as that of the ion emitting anode. This voltage arrangement results in curved equipotential surfaces near the anode so that the beam sees a very strong radial focusing force near the ion emitting surface and the first electrode. The beam is pinched and focused roughly to a 1mm radius spot size at the injector exit. The space-charge limited current is then reduced. Since the beam radius is much smaller than the electrodes' aperture size, the external field beam sees is very linear. There is no normalized emittance growth in this case. The radial mesh size used in the simulation was quite coarse ($\Delta r = 0.6$ mm) compared with the 1 mm beam radius. There is not enough resolution to simulate the small beam size and beam divergence properly. Nevertheless, we have obtained very good

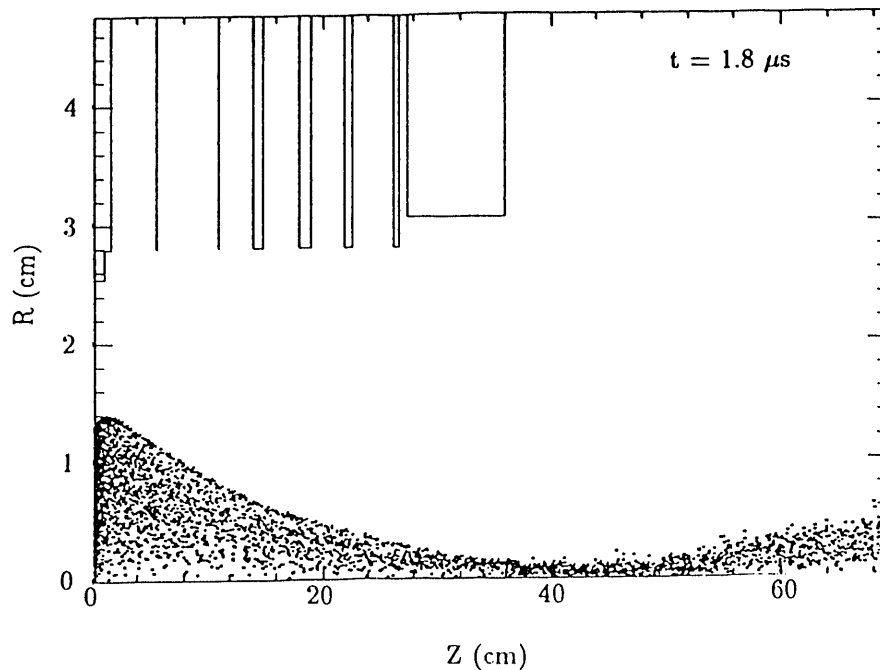


Fig. 4 The LBL HIF injector without a current valve

agreement in the values of current and normalized emittance with experiments and EGUN calculations as given in Table II.

Table II The LBL HIF injector without a current valve

	GYMNOS	EXP ⁶	EGUN ⁷
Current (mA)	20	> 24	19
Normalized emittance (mm-mr)	.06	.04	0.05
Beam radius (mm)	5.0	1.2	0.9
Beam divergence (mr)	19	6	8

SUMMARY

We have developed and implemented a space charge emission algorithm to the time dependent axisymmetric PIC code, GYM-NOS. The algorithm can provide the correct Child-Langmuir current when the number of mesh points in the A-K gap is as little as 8. Comparing with the analytic results, the simulation can also provide the predicted transient behavior. Finally, the GYM-NOS simulations of the LBL HIF electrostatic column injector agree with the experimental data and EGUN results quite well.

ACKNOLEGEMENT

The authors would like to thank S.S. Yu and J.J. Barnard for their useful discussions during the course of this study.

REFERENCES

1. W.B. Herrmannsfeldt, "Electron Trajectory Program", SLAC Report No. SLAC-226, UC-28 (A), Nov. 1979.
2. D.W. Hewett and D.J. Larson, "The Best of GYM-NOS: A User's Guide", LLNL Report No. UCRL-ID-110499, May 4, 1992.
3. Lample and Tiefenback, Appl. Phys. Lett. Vol. 43, No. 1, p. 1 (1983).
4. H.L. Rutkowski, D.W. Hewett, and S. Humphries Jr., "Development of Arc Ion Sources for Heavy Ion Fusion", IEEE Transactions on Plasma Science, 19, No. 5, Pg. 782 (1991).
5. D.W. Hewett, M.R. Gibbons, and H.L. Rutkowski, "Extracting Low Emittance Ion Beams through a Current Valve/Switch Mesh", (in preparation, 1993).
6. S. Eylon, private communication, (1992).
7. E. Henestroza, private communication, (1993).

END

**DATE
FILMED**

10/01/93

